Search for an Annual Modulation in a *p*-Type Point Contact Germanium Dark Matter Detector

C. E. Aalseth,[1] P. S. Barbeau,[2,*] J. Colaresi,[3] J. I. Collar,[2,†] J. Diaz Leon,[4] J. E. Fast,[1] N. Fields,[2]
T. W. Hossbach,[1,2] M. E. Keillor,[1] J. D. Kephart,[1] A. Knecht,[4] M. G. Marino,[4,‡] H. S. Miley,[1]
M. L. Miller,[4] J. L. Orrell,[1] D. C. Radford,[5] J. F. Wilkerson,[6] and K. M. Yocum[3]

(CoGeNT Collaboration)

[1]*Pacific Northwest National Laboratory, Richland, Washington 99352, USA*
[2]*Kavli Institute for Cosmological Physics and Enrico Fermi Institute, University of Chicago, Chicago, Illinois 60637, USA*
[3]*CANBERRA Industries, Meriden, Connecticut 06450, USA*
[4]*Center for Experimental Nuclear Physics and Astrophysics and Department of Physics, University of Washington,
Seattle, Washington 98195, USA*
[5]*Oak Ridge National Laboratory, Oak Ridge, Tennessee 37831, USA*
[6]*Department of Physics and Astronomy, University of North Carolina, North Carolina 27599, USA*

Fifteen months of cumulative CoGeNT data are examined for indications of an annual modulation, a predicted signature of weakly interacting massive particle (WIMP) interactions. Presently available data support the presence of a modulated component of unknown origin, with parameters *prima facie* compatible with a galactic halo composed of light-mass WIMPs. Unoptimized estimators yield a statistical significance for a modulation of $\sim 2.8\sigma$, limited by the short exposure.

CoGeNT employs *P*-type Point Contact (PPC) germanium detectors [1–3] to explore light-mass WIMP dark matter models. By virtue of their low electronic noise, PPCs are ideal for searches in the mass range $m_\chi < 10\ \mathrm{GeV}/c^2$. Their ability to reject background events taking place on detector surfaces is described in [1]. Prompted by the interruption in data taking imposed by a recent fire in the access shaft to the Soudan Underground Laboratory (SUL), we have examined existing CoGeNT data for the presence of an annual modulation in the WIMP interaction rate [4]. The characteristics of this detector, data analysis and background interpretations are treated in a recent Letter [1], to which the reader is referred.

Underground installation of this PPC at SUL took place on August 21, 2009. Following an upgrade to the data acquisition to allow discrimination of surface events, data-taking started on December 4th, a date close to the minimum in rate expected from the annual modulation effect [4]. Data taking was interrupted exclusively over the periods of February 9–15, March 15–20, and October 5–7 of 2010, for inspection of a higher-energy region of the spectrum and two planned general power outages at SUL. The data set presented here ends on March 6 of 2011, spanning 458 days, of which 442 were live. On this date the detector was stopped for another planned outage. Outage-related computer problems delayed normal operation until two days before the fire (March 17, 2011).

Surface background- and microphonic-rejection cuts on these data are as in [1], and constant in time. An alternative analysis [5] results into very similar conclusions, to be

treated elsewhere [6]. In the following discussion, the astrophysical halo parameters in [7,8] are used.

Figure 1 (top) displays spectral peaks appearing at the *K*-shell binding energy of daughters of cosmogenically activated radio isotopes decaying via electron capture (EC) [1]. The bottom panel in the same figure zooms in to the lower-energy region of the spectrum, down to the $\sim 0.5\ \mathrm{keV}_{ee}$ (keV electron equivalent or ionization energy) threshold. A fit to the evolution of the *K*-shell peaks returns excellent agreement with the expected half-lives and allows a prediction for the initial abundance of these radio isotopes with individual uncertainty of O(10)%. The ratio between *L*-shell and *K*-shell EC is well defined for these isotopes, both theoretically and experimentally [9]. It can be used to generate a prediction, devoid of any free parameters, for the intensity of the *L*-shell peaks in this lower-energy spectrum (Gaussians in Fig. 1, bottom). After subtraction of this predicted *L*-shell EC contribution and of a constant spectral component, and following the correction for the combined trigger and software-cut efficiency [1], an exponential-like irreducible background of events taking place in the bulk of the crystal is observed (Fig. 1, inset). These events are individually distinct from any identifiable source of noise, display the characteristics (rise and decay time) of radiation-induced pulses, and have a uniform diurnal distribution. Predicted signals from example combinations of light-WIMP masses and spin-independent WIMP-nuclei couplings are also shown as a reference.

Black dots in the inset of Fig. 1 represent the irreducible spectrum obtained by stripping of the *L*-shell predictions
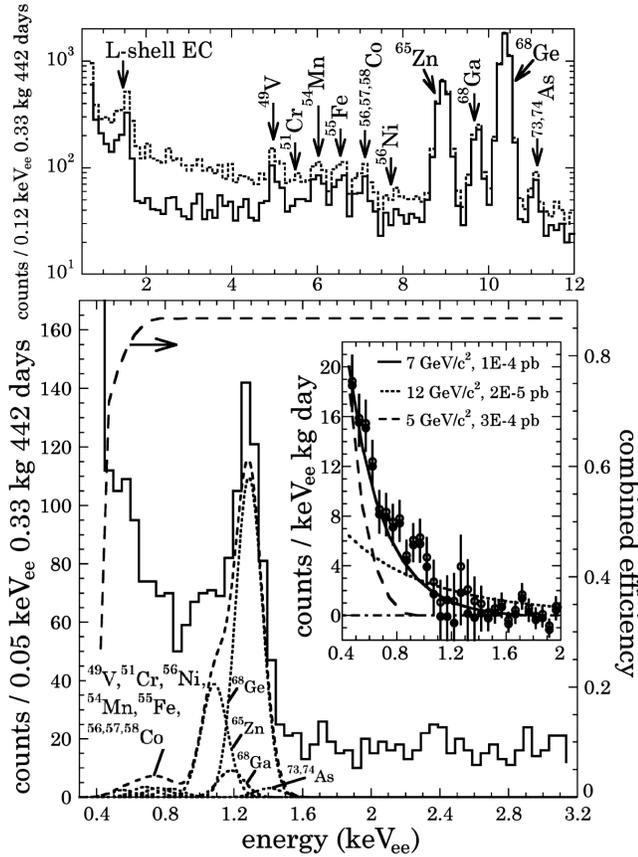
FIG. 1. Top: Uncorrected (i.e., prior to threshold efficiency correction) spectrum displaying all expected K-shell EC cosmogenic peak positions. The dotted histogram shows the spectrum before rejection of surface background events. Bottom: Uncorrected low-energy spectrum following removal of surface events. Dotted Gaussian peaks show the predicted L-shell EC contribution, devoid of any free parameters (see text). A dashed line traces their envelope. A second dashed line indicates the combined threshold efficiency (trigger + software cuts) [1], an arrow pointing from it to the right scale. Inset: Spectra corrected by this efficiency and stripped of L-shell contribution and flat background component. Examples of light-WIMP signals are overlapped on it (see text).

and the flat background level in the region $\sim$2–4.5 keV$_{ee}$. Unfilled circles are obtained when a free overall normalization factor multiplies the envelope of the individual L-shell predictions in a background model containing this envelope, an exponential and a constant background. The resulting best-fit indicates a L-shell contribution just 10% short of the nominal prediction, well within its uncertainty. Figure 2 shows the region of interest (ROI) obtained when these irreducible spectra are fitted by a sample model containing signals from WIMPs of mass m_χ and spin-independent coupling σ_{SI}, and a free exponential background. As in [1], this ROI is defined by the upper and lower 90% C.L. intervals for the best-fit σ_{SI}, whenever the lower interval is incompatible with a null value. This ROI is meant to direct the eye to the region of
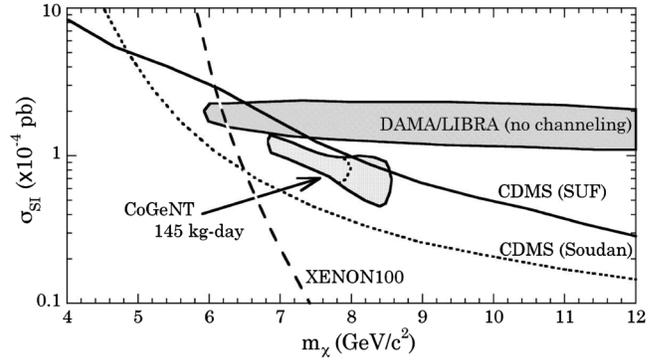

FIG. 2. ROI extracted from the irreducible spectra in Fig. 1 (inset) under consideration of a light-WIMP hypothesis. A small dotted line bisects it, approximately separating the domains favored by the black dot (left) or unfilled circle (right) spectra in Fig. 1. ROI definition and uncertainties able to shift it are described in the text. The DAMA/LIBRA ROI includes present uncertainties in its position [11], with the exception of ion channeling [27], conservatively assumed to be absent. Solid and dotted lines are CDMS limits from [7,28], respectively. A dashed line corresponds to recent XENON100 claims [8]. Uncertainties in these constraints and those by XENON10 [24] are examined in [22,25].

parameter space where the hypothesis of a WIMP signal dominating the irreducible background events fares best, but it does not include astrophysical or other uncertainties listed next. Reasonable uncertainties in the germanium quenching factor employed (Fig. 4 in [2], [10]) can shift this ROI by $\sim \pm 1$ GeV/c^2. The present uncertainty in the fiducial bulk volume of this detector is O(10)% [1]. Departures from the assumption of a constant background in the model above can also displace this region. A modest contamination of the spectrum by surface events next to threshold [1,6] would shift this ROI to slightly higher values of m_χ and lower σ_{SI}. The additional exposure collected since [1] results in a much reduced CoGeNT ROI, one in the immediate vicinity of the parameter space compatible with the annual modulation effect observed by DAMA/LIBRA [11,12]. This region of σ_{SI}, m_χ space is populated by the predictions of several particle phenomenologies. The reader is directed to references in [1] and recent literature for examples. The same region has received recent attention within the context of dark matter annihilation signatures at the center of our Galaxy, and anomalies in accelerator experiments [13]. Figure 2 also displays limits from other searches, a subject treated again below.

A search for a WIMP-induced annual modulation in dark matter detector data requires an exceptional low-energy stability in the device. Figure 3 shows that these conditions are present for CoGeNT. The top panel displays daily averages in the detector electronic noise. Excessive excursions in this parameter would affect the stability of the detector threshold. These are not observed. Precautions
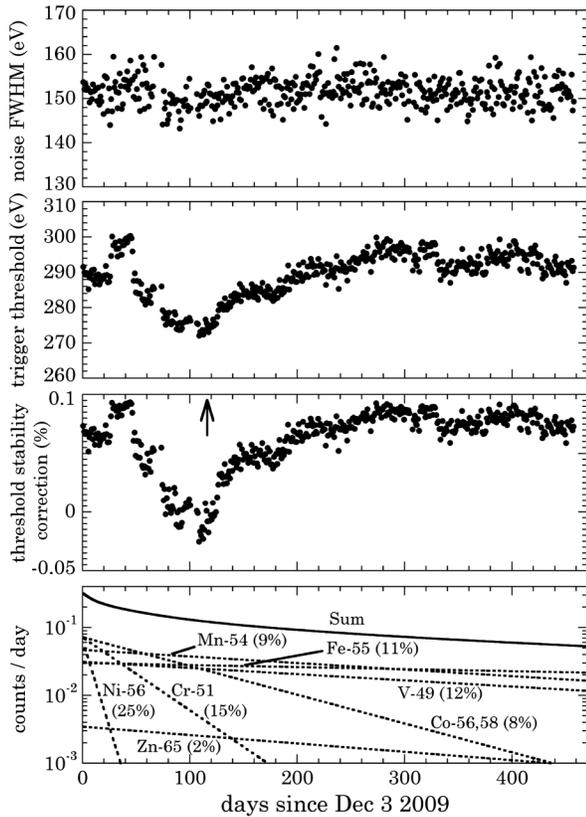
FIG. 3. Assessment of the stability of the CoGeNT PPC at Soudan (see text). First panel: daily average in detector electronic noise (shaping time 10 μs). Second panel: stability of the trigger threshold level. Third panel: negligible correction to the counting rate in the region 0.5–0.9 keV$_{ee}$ induced by it. Fourth panel: expected counting rate in this same region originating in L-shell EC. The observed stability augurs well for WIMP modulation searches using next-generation PPCs like those planned for the upcoming expansion of CoGeNT (C-4), MAJORANA, GERDA, and CDEX.
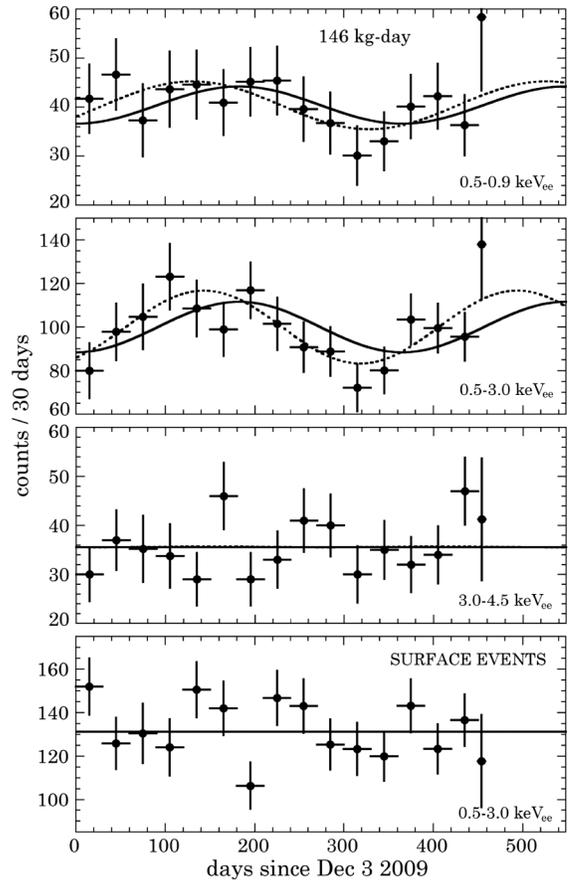

FIG. 4. Rate vs time in several energy regions (the last bin spans 8 days). A dotted line denotes the best-fit modulation. A solid line indicates a prediction for a 7 GeV/c^2 WIMP in a galactic halo with Maxwellian velocity distribution. Background contamination and/or a non-Maxwellian halo can shift the amplitude of this nominal modulation (see text). Dotted and solid lines overlap for the bottom panels.

are taken to ensure that this noise is as stable as possible: for instance, by automatically refilling the detector liquid nitrogen Dewar every 48 h, the crystal temperature and its associated leakage current are held as constant as possible. The second panel shows the stability of the trigger threshold, derived from the difference between the daily average baseline DC level in the triggering channel and a constant (digitally fixed) discriminator level. The small excursions observed correspond to a temperature drift in the digitizers (NI 5102) and shaping amplifier (Ortec 672) of ~1° C. These small instabilities do not result in any minor smearing of the energy resolution, given that the amplitude of each event is referenced to its individual pretrigger DC level. The effect of this small baseline drift should instead be envisioned as a maximum shift of the threshold efficiency curve in Fig. 1 by about ±10 eV. The third panel shows the calculation of by how much such a shift can affect the counting rate in the region 0.5–0.9 keV$_{ee}$. This calculation includes the exponential spectral shape

observed there. The correction is referenced to the date of the threshold efficiency calibration employed (small arrow in Fig. 3) and found to be negligible at less than 0.1%. This correction would be larger for events below 0.5 keV$_{ee}$, not considered here, and even smaller for count rates in broader energy regions starting at 0.5 keV$_{ee}$. The fourth panel indicates the magnitude of the correction required to account for the exponential decay of L-shell EC radio isotopes, prior to an annual modulation analysis. This correction affects the 0.4–1.6 keV$_{ee}$ region (Fig. 1), where a light-WIMP can express a modulated signature. The uncertainties in this correction, indicated in Fig. 3 in parentheses, are modest even at the present exposure. A direct comparison of these predictions with the low-energy spectrum, as done in Fig. 1, demonstrates that they are robust.

Figure 4 shows the temporal rate behavior in several spectral regions following the correction for L-shell EC activity, when applicable. Even with the present limited exposure, a noticeable annual modulation can be observed

in the energy region encompassing the exponential rise in irreducible background in Fig. 1. The statistical significance for this modulation is presently maximal for an energy bin ranging from threshold ($0.5\ keV_{ee}$) to an upper bracket anywhere in the interval ~ 2.0–$3.0\ keV_{ee}$ (the amplitude of a WIMP-induced modulation is expected to be maximal towards its spectral endpoint [14,15]). No indication of a modulation is observed above this energy, nor for events rejected as surface backgrounds in the same spectral region where it is the largest for bulk events (bottom panel in Fig. 4). The "internal clock" provided by the most intense K-shell peak at $10.37\ keV_{ee}$ exhibits no modulated deviation from an exponential decay, nor any significant time-dependent changes in mean energy.

Ad hoc methods able to extricate a modulated component with maximal sensitivity [15] have not been attempted. A few considerably less sensitive indicators of modulation significance are presently offered. For instance, for the region 0.5–$3.0\ keV_{ee}$ and (unoptimized) binning depicted in Fig. 4, a straightforward analysis reveals a reduced chi-square $\chi^2/\text{d.o.f.} = 7.8/12$ (80% C.L. for acceptance) for the best-fit modulation. The null hypothesis (absence of a modulation) fares considerably worse at $\chi^2/\text{d.o.f.} = 20.3/15$ (84% C.L. for rejection). The likelihood ratio test indicates that the modulation hypothesis is preferred over the null hypothesis at 99.4% C.L. (2.8σ). Intriguingly, the best-fit values for the three modulation parameters ($16.6 \pm 3.8\%$ modulation amplitude, period 347 ± 29 d, minimum in Oct. 16 ± 12 d) do not fall far from the predictions provided by the WIMP hypothesis (a calculable amplitude, a yearly period and minimum amplitude in late Nov. to early Dec. [16]). The most uncertain of these predictions [16,17], the amplitude, is derived as in [14], including the dependence on astrophysical parameters, target, threshold, WIMP mass, etc., For $m_\chi = 7\ \text{GeV}/c^2$ an expected value of 12.8% is obtained (Fig. 4). While the apparent DAMA/LIBRA modulation is weaker ($\sim 2\%$ of the low-energy rate), its enhancement for CoGeNT is expected in most light-WIMP scenarios [17,18]. If these predictions are accepted, the Monte Carlo probability of better simultaneous agreement with them than that provided by the best-fit values above, is small at 0.7%, for simulated random fluctuations around the 0.5–$3.0\ keV_{ee}$ mean rate.

In addition to the basic estimators presented here, time-stamped CoGeNT data are available by request. These can be used not only for alternative analyses of significance, etc., but also to investigate noncosmological effects that might generate this modulation and by extension that observed by DAMA/LIBRA. In this respect, the muon flux at SUL varies seasonally by $\pm 2\%$, and radon levels by a factor ~ 4 [19]. Muon-coincident events constitute a few percent of the low-energy spectrum [1], limiting a muon-induced modulated amplitude to $\ll 1\%$ [6]. Rejection of veto-coincident events does not alter the observed modulation. Radon displacement via pressurized LN boil-off gas is continuously maintained at $2\ l/\text{min}$ within an aluminum shell encasing the lead shielding [20]. A radon-induced modulation would be expected to affect a much broader spectral region than observed [21].

The CDMS collaboration has recently claimed [7] to exclude a light-WIMP interpretation of CoGeNT and DAMA/LIBRA observations. Uncertainties affecting this claim are discussed in [22,23]. Observations from XENON10 [24] and XENON100 [8] have been used to claim a similar rejection of light-WIMP scenarios. Uncertainties affecting these searches are examined in [25].

In conclusion, presently available CoGeNT data favor the presence of an annual modulation in the low-energy spectral rate, for events taking place in the bulk of the detector only. While its origin is presently unknown, the spectral and temporal information are *prima facie* congruent when the WIMP hypothesis is examined: in particular, the WIMP mass region most favored by a spectral analysis (Fig. 2) generates predictions for the modulated amplitude in agreement with observations, modulo the dependence of this assertion on the choice of astrophysical parameters and halo velocity distribution [16–18,26].

---

*Present address: Department of Physics, Stanford University, Stanford, CA 94305, USA.
†Corresponding author.
collar@uchicago.edu
‡Present address: Physics Department, Technische Universität München, Munich, Germany.

[1] C. E. Aalseth *et al.*, Phys. Rev. Lett. **106**, 131301 (2011).
[2] P. S. Barbeau, J. I. Collar, and O. Tench, J. Cosmol. Astropart. Phys. 09 (2007) 009.
[3] C. E. Aalseth *et al.*, Phys. Rev. Lett. **101**, 251301 (2008); **102**, 109903(E) (2009).
[4] A. K. Drukier, K. Freese, and D. N. Spergel, Phys. Rev. D **33**, 3495 (1986).
[5] M. G. Marino, Ph.D. Diss., Univ. of Washington, 2010.
[6] CoGeNT collaboration (to be published).
[7] Z. Ahmed *et al.*, Phys. Rev. Lett. **106**, 131302 (2011).
[8] E. Aprile *et al.*, arXiv:1104.2549.
[9] J. N. Bahcall, Phys. Rev. **132**, 362 (1963).
[10] P. S. Barbeau, Ph.D. thesis, University of Chicago, 2009.
[11] D. Hooper *et al.*, Phys. Rev. D **82**, 123509 (2010).
[12] R. Bernabei *et al.*, Eur. Phys. J. C **56**, 333 (2008).
[13] D. Hooper and L. Goodenough, Phys. Lett. B **697**, 412 (2011); D. Hooper and T. Linden, Phys. Rev. D **83**, 083517 (2011); M. R. Buckley *et al.*, Phys. Lett. B **702**, 256

(2011); Phys. Rev. D **83**, 115013 (2011); P. J. Fox *et al.*, arXiv:1104.4127.

[14] J. D. Lewin and P. F. Smith, Astropart. Phys. **6**, 87 (1996).

[15] K. Freese, J. Frieman, and A. Gould, Phys. Rev. D **37**, 3388 (1988).

[16] M. Kuhlen *et al.*, J. Cosmol. Astropart. Phys. 02 (2010) 030.

[17] P. J. Fox, J. Liu, and N. Weiner, Phys. Rev. D **83**, 103514 (2011).

[18] C. Kelso and D. Hooper, J. Cosmol. Astropart. Phys. 02 (2011) 002.

[19] M. Goodman, *Proceedings of the 26th Intl. Cosmic Ray Conf., Aug. 17-25, Salt Lake City, Utah*.

[20] http://cogent.pnnl.gov/gallery.stm

[21] G. Heusser *et al.*, Appl. Radiat. Isot. **43**, 9 (1992).

[22] J. I. Collar, arXiv:1103.3481.

[23] Z. Ahmed *et al.*, arXiv:1011.2482v3.

[24] J. Angle *et al.*, Phys. Rev. Lett. **107**, 051301 (2011).

[25] J. I. Collar, arXiv:1106.0653.

[26] M. Lisanti *et al.*, Phys. Rev. D **83**, 023519 (2011).

[27] N. Bozorgnia, G. B. Gelmini, and P. Gondolo, J. Cosmol. Astropart. Phys. 11 (2010) 019.

[28] D. S. Akerib *et al.*, Phys. Rev. D **82**, 122004 (2010).